

Inspection of Arc Trails Formed in Stellarator/Heliotron Devices W7-X and LHD^{*})

Dogyun HWANGBO^{a)}, Shin KAJITA¹⁾, Chandra Prakash DHARD²⁾, Masayuki TOKITANI³⁾, Marco KRAUSE²⁾, Dirk NAUJOKS²⁾, Suguru MASUZAKI³⁾, Sören KLOSE²⁾, Noriyasu OHNO and The W7-X Team²⁾

Graduate School of Engineering, Nagoya University, Nagoya 464-8603, Japan

¹⁾*Institute of Materials and Systems for Sustainability, Nagoya University, Nagoya 464-8603, Japan*

²⁾*Max-Planck Institute for Plasma Physics, Wendelsteinstrasse 1, 17491 Greifswald, Germany*

³⁾*National Institute for Fusion Science, National Institutes of Natural Sciences, Toki 509-5292, Japan*

(Received 28 November 2019 / Accepted 22 February 2020)

Arc trails found in heliotron/stellarator devices Large Helical Device (LHD) and Wendelstein 7-X (W7-X) were inspected; arcing occurred on different locations at various situations. In LHD, a helium-plasma-induced tungsten nanostructure sample was installed and exposed to a LHD plasma. Many arc trails were formed only on the sample with nanostructures, suggesting an easy initiation of arcing compared to pristine tungsten. After the completion of annual campaign 2011 in LHD, arc trails appeared on a graphite divertor tile which was taken out for inspection. Because the arc trails had a linear shape, the arcing was likely caused by main discharge operation. In W7-X, some Langmuir-probes installed within the limiter tiles suffered severe damage with arc trails during the operational phase 1.1. After the operational phase 1.2b, in-vessel inspection was performed for the first time for all the plasma facing components focused on arcing. No arc trails appeared on graphite components including test divertor units. In turn, considerable number of the trails appeared on non-plasma exposed region. Most of the arc trails had no clear linearity, indicating that arcing initiated during glow discharge cleaning phase. Only a few trails seemed to be affected by the existence of an external magnetic field. A vast majority (80%) of arcs were initiated from the edge of surfaces, while half of arc trails starting on the interior region of surfaces were accompanied by deposition spots. Broad arc trails appeared on the surfaces of diagnostic ports and mirrors.

© 2020 The Japan Society of Plasma Science and Nuclear Fusion Research

Keywords: Large Helical Device, Wendelstein 7-X, plasma surface interaction, arcing, tungsten fuzz

DOI: 10.1585/pfr.15.2402012

1. Introduction

Emerging trends toward high-confinement operations of large-scale fusion devices make arcing on plasma-facing components (PFCs) revisited as an interest of wall erosion and impurity releasing source since it had been actively studied in 1980s [1]. For a recent decade, many researches have been dedicated to evaluate the amount of erosion of PFCs due to arcing in controlled manners [2–4]. Most of those researches were performed in large-scale tokamaks, where periodic transient heat loads such as edge localized modes (ELMs) are expected, because the potential drop and the electric field between the plasma and the wall increase greatly during the ELMs, which is favourable for an arc ignition.

Arcing also delivers harmful effects to diagnostic systems equipped in fusion devices as previous researches have reported arcing on: retroreflector surfaces in LHD [5]

and a outer-vessel mirror surface of Thomson scattering diagnostics in JT-60U [6]. These surface damages degrades the precision of measurements and therefore arcing on diagnostics should be prevented.

In addition, helium (He)-induced nanostructuring of tungsten (W), which is considered the most promising material for the divertor, can increase the possibility of arc ignition on wall surfaces of future fusion reactors. Fiber-formed nanostructure of W, so-called W-fuzz, is predicted to grow on the outer divertor target of ITER [7], where the surface temperature and the incident ion energy sufficiently meet the formation condition for the W-fuzz [8]. Owing to drastic changes in thermal and electrical properties of a W-fuzz surface [9, 10], it is now well known that an arc easily ignites on W-fuzz under the exposure of edge plasmas, which was already demonstrated in LHD [11], DIII-D [12] and COMPASS [13].

In helical devices, where no transient heat loads are expected, arc trails were observed on either W-fuzz surfaces [11] or deposited layers of a divertor module and retroreflector surfaces [5, 14]. Thus far, arcing has not

^{a)} current affiliation: Faculty of Pure and Applied Science, University of Tsukuba, Ibaraki 305-8577, Japan

author's e-mail: hwangbo.dogyun@gmail.com

^{*}) This article is based on the presentation at the 28th International Toki Conference on Plasma and Fusion Research (ITC28).

been included in the framework of plasma-wall interaction (PWI) research in fusion devices, primarily due to lack of statistical analysis. Arcing's irregular, pulsed and localized nature has made researchers difficult to clarify the ignition mechanism and quantify its effects. Thus, statistical assessment of the likelihood of arcing is urgent to estimate the amount of erosion and reflect the potential effects of arc ignition on PWI researches. In this paper, arc trails formed in two stellarator/heliotron devices W7-X and LHD were inspected. Arc trails on a W-fuzz surface under LHD plasma exposure are analyzed to reveal the effect of surface nanostructuring on arc ignition. Several PFCs of LHD were taken out of the vacuum vessel and inspected to detect arc trails. For W7-X, arc trails formed on Langmuir probes equipped in limiter tiles during the operation phase 1.1 (OP 1.1) were analyzed. After the OP 1.2b, an in-vessel inspection was performed for the first time mainly focused on arc trails for spatial distribution and quantitative analysis.

2. Arcing Initiated in LHD

2.1 Arcing on a W-fuzz

Two W samples ($10 \times 80 \times 3 \text{ mm}^3$) were prepared and one was exposed to a He plasma of the linear magnetized divertor simulator NAGDIS-II (Nagoya Divertor Simulator) for W-fuzz formation on the surface (W-fuzz in Fig. 1 (a)). The exposure followed the formation condition of fuzz [8] and the ion fluence ($\sim 10^{25} \text{ m}^{-2}$) was set to give approximate W-fuzz thickness of $1.4 \mu\text{m}$. Figure 1 (b) shows a scanning electron microscopic (SEM) image of the W-fuzz sample, which presents typical fuzz growth on the surface. The other was kept pristine as a control (Virgin W in Fig. 1 (a)). The samples were installed on a sample holder and then inserted inside the vacuum vessel of LHD. Figure 1 (a) shows a schematic sketch of the W-fuzz manipulator probe. The samples were electrically isolated from the sample holder. The sample surfaces were tilted 5° from the orientation of magnetic field lines. The experiment was performed for one hydrogen discharge. The discharge duration was $\sim 1.5 \text{ s}$ and the electron density at the core was $3 - 4 \times 10^{19} \text{ m}^{-3}$. Magnetic field at core was the 2.75 T.

As a result, arcs ignited on the W-fuzz surface but not on the virgin W. Figure 2 (a) shows a digital microscope image of arc trails occurred on the W-fuzz surface. In total 18 trails were observed and they propagated along the opposite direction of the cross product of arc current and external magnetic field line $-\mathbf{j} \times \mathbf{B}$, so-called retrograde direction. Owing to much stronger magnetic field, the arc trails appeared with clear lines, which are different from the previous result showing zigzag motion at tenfold lower magnetic field [15].

Previously, W-fuzz samples were installed in LHD and an arcing occurred on its surface [11, 14]. The sample surfaces were oriented perpendicular to the magnetic

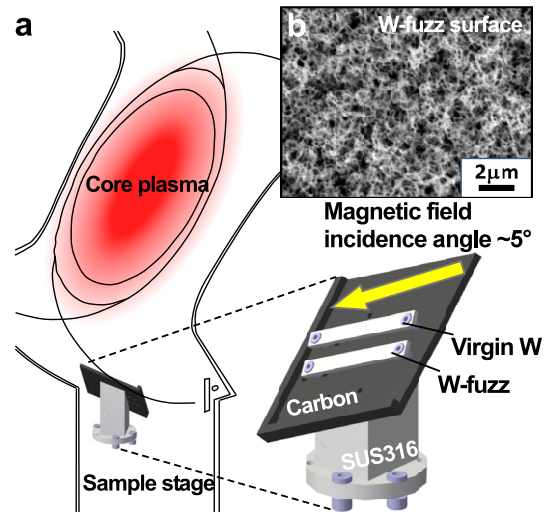


Fig. 1 (a) A schematic sketch of a W-fuzz sample mounted on a manipulator probe in LHD (b) an SEM micrograph of the W-fuzz sample.

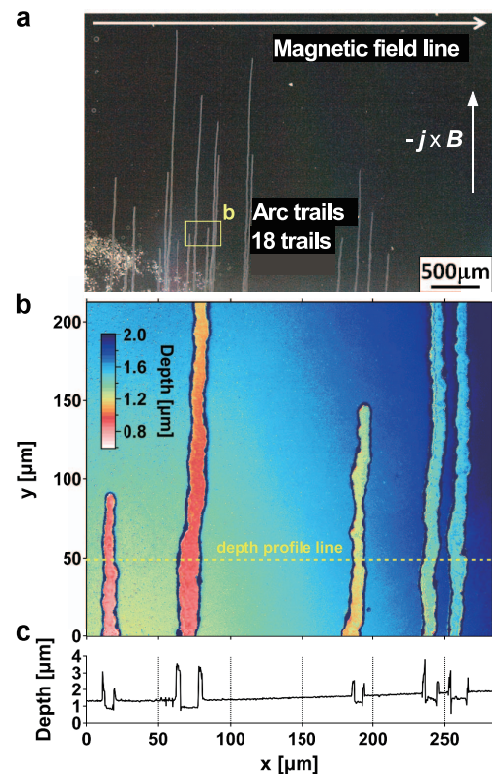


Fig. 2 (a) A digital microscope image of arc trails remained on the W-fuzz surface, (b) a depth profile of several arc trails marked in (a), and (c) a depth line profile dashed in (b).

field lines. Thus, there was no effective $-\mathbf{j} \times \mathbf{B}$ directivity and the arc spots moved in a random manner. Considering the small contained angle (several degree) between a divertor surface and incident magnetic field lines in future devices like ITER [16], the straightforward arc trails in this research suggests probable movement of arc spots in the divertor modules. It should be noted that there was

no arc trails on the virgin W surface and that the arcs ignited even without exposing the W-fuzz surface to a transient high heat load. This implies that W-fuzz can act as an initiator of arcing on future devices, where partially higher heat load would be expected on wall surfaces.

To estimate the erosion depth by the arcing, confocal laser microscopy was performed with the horizontal and vertical pitches of 277 nm/pixel and 100 nm/step, respectively. Figure 2(b) shows a depth profile of several arc trails. The region of interest is marked in Fig. 2(a). The width of the arc trails ranged 5-12 μm . Colorized trails clearly show that the arc trails were dented compared to the surrounding surface. Figure 2(c) shows a line depth profile at $y = 50\mu\text{m}$ in Fig. 2(b). Considering the gradient bulk surface, typical erosion depth by arcing was $\sim 0.4\mu\text{m}$. It is worth noted that the surrounding W-fuzz area was damaged by the plasma exposure, thus becoming thinner than the initial state of $\sim 1.4\mu\text{m}$. Compared to the previous research [11, 14], the erosion area appeared to be much smaller. One factor is linearity of motion, which reduced chances for the arc spots to stay longer around the surface. In addition, post-mortem observation confirmed that the strike-point of the plasma lied on an edge of the sample, implying lessened heat influx toward the fuzzy layer. From the Fig. 2, mass erosion by arcing was estimated as $\sim 0.5\mu\text{g}$. A vast majority of eroded materials were redeposited to the vicinity of the arc trails, as seen in Fig. 2(c). In addition to the small area eroded, this also resulted in smaller mass erosion compared to the previous research [14]. It is noteworthy that these arcs had mere effects on the plasma discharge and the discharge ended safely as planned.

2.2 Arcing on plasma facing components

After the operation year 2011, several in-vessel components were taken out for inspection. Some were introduced already in the previous report [14], in which arc trails on an ECH mirror rear-side surface and a first wall panel were observed. Arc trails were also discovered on the other surfaces. Figure 3(a) shows an arc trail formed on the side surface of an ECH mirror. The arc trails were recorded broadly with area of roughly $\sim 1200\text{mm}^2$ and the morphology was not linear, indicating that the arc ignited in a non-magnetized environment.

Arc trails were also observed on a divertor module surface. Figure 3(b) shows a digital microscope image of arc trails recorded on a deposition layer of a divertor module. Several trails appear and the trail patterns show a certain orientation that is close to $-\mathbf{j} \times \mathbf{B}$ direction, implying that the arcing was initiated during main discharge under a strong magnetic field. Slight tilted propagation is likely because the surface normal was not exactly perpendicular to the magnetic field line that leads to tilted propagation of arc spots following the acute angle rule [17].

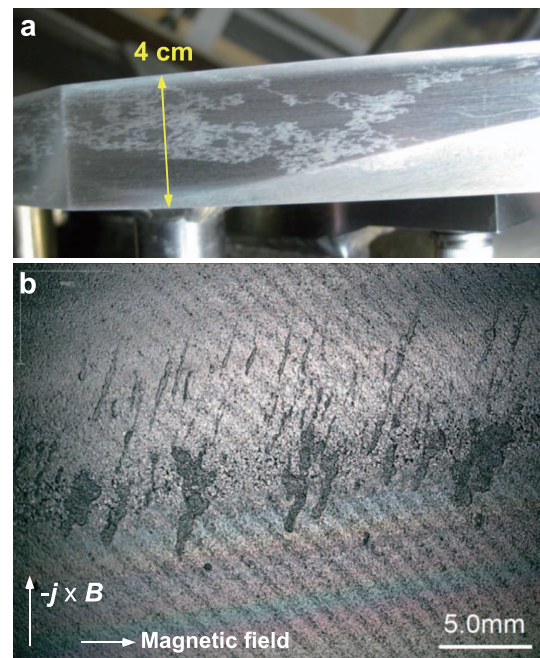


Fig. 3 (a) A photo of an arc trail on the side surface of an ECH mirror and (b) a digital microscope image of arc trails on a deposition layer of a divertor module.

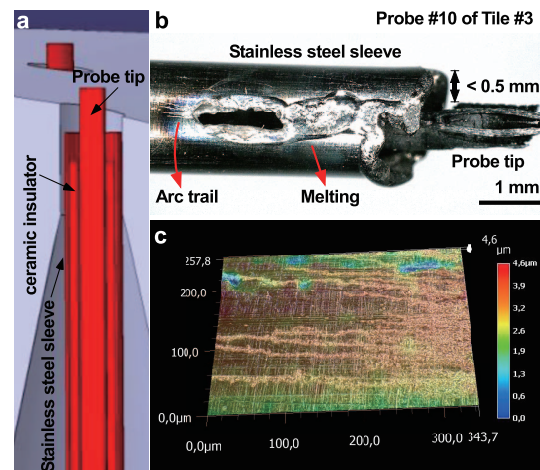


Fig. 4 (a) An illustration of the limiter module Langmuir probe, (b) a photo of a probe set with a damage on its graphite tip and a stainless sleeve and (c) a depth profile of the arc trail in (b). Note that the gray color image is superpositioned with the depth profile.

3. Arcing Initiated in W7-X

3.1 Arcing on Langmuir probe after OP 1.1

After the first operation phase of W7-X (OP 1.1) Langmuir probes integrated into the limiter of module 5 were taken out together with the limiters from other four for inspection. The probe system consists of an upper and a lower array of 20 probe tips each (See Fig. 1 in [18]). As shown in Fig. 4(a), cylindrical graphite tips with a diameter of 0.9 mm were inserted into stainless steel (SS) sleeves

with a gap of < 0.5 mm in between filled by ceramic insulators. The tips were either flush mounted or stuck out of the limiter surface by 1 mm [19].

Among 40 probes in total, 4 probe tips suffered damages. Figure 4 (b) shows a photo of a damaged probe tip with melted SS sleeve. The graphite tip seemingly evaporated. On the SS sleeve, typical cathodic arc trails also appeared. The SS sleeve melting was primarily due to concentration of high current because of lack of in-built fuses in the power supplies. Figure 4(c) shows a depth profile of the arc trail by profilometry. A color scale bar indicates the height of the surface, which ranged 0 - 4.6 μm . The erosion depths of the trails were ~ 1 μm , which were smaller than the depths of arc spots in a previous study, which presented 4 - 40 μm of erosion depths on P92, martensitic-ferritic high temperature steel inserts in ASDEX-U [3].

Considering that graphite can evaporate when playing as an anode, arc ignition seemed to occur between the probe tip and the SS sleeve. However, at this moment it is unclear what originated such high current. It is worth noted that there was a blank space where the ceramic insulator was not filled between the probe tip and SS sleeve (See Fig. 4 (a)). The SS sleeves were grounded with the limiter modules, thus there was a triple metal-dielectric-vacuum junction, which usually regarded as the most common way of initiating vacuum breakdown [20]. Operational voltage range of the probe was ± 200 V [19]. It allowed the maximum electric field of 0.4 kV/mm between the probe rod and the SS sleeve with the gap distance 0.5 mm, however, which is yet lower than the minimal value generally required for vacuum breakdown of several kV/mm with the triple junction [21].

An increase in neutral gas pressure could lead to lower breakdown voltage. In this study, neutral pressure in near-divertor region of W7-X varied throughout the campaign. One can notice that the neutral pressure at sub-divertor region marked $3 - 5 \times 10^{-3}$ Pa with pulsed divertor fueling phase [22], which would be regarded as rather high level in the total range of neutral pressure available. According to [23], flashover voltages on insulators with atmospheric air decreased by one fourths compared to high vacuum cases. However, the voltages stayed unchanged when the gas pressure was upto ~ 0.1 Pa.

The SS sleeve has edge parts and the electric field can be enhanced. In general field enhancement factor can be roughly calculated with a geometry of tip. Considering the ratio of the thickness and height of the SS sleeve, field enhancement factor is given ~ 10 , which still gives a local electric field far below the threshold for vacuum breakdown of several tens kV/mm [20]. It is also valuable to consider the effect of surface charge at an insulator. In Fig. 4 (b), melting started from the junction between the insulator and the SS sleeve. Near-cathode surface of insulators could be charged positively, then incident electrons can be accelerated into the surface of insulators and produce more secondary electrons, resulting in secondary

electron emission avalanche and flashover [21].

One can also consider the effect of plasma exposure. The SS sleeve and the insulator were inserted below the limiter surface by several mm and the strong magnetic field of 2.5 T existed, which gives the gyroradius of a hydrogen ion ~ 0.1 mm, so that direct impacts of W7-X plasmas were not likely. Instead, smaller portion of plasmas with low temperature and density could exist in this sub-surface, affecting the electric field between two electrodes. To clarify the mechanism of the melting and the arcing, detailed analysis of current-voltage characteristics of the probe systems is needed to detect whether extraordinary increases in probe current were observed, and specify corresponding discharge conditions.

3.2 In-vessel inspection after OP 1.2b

During the second operational phases (OP 1.2a and 1.2b) of W7-X, passively cooled test divertor units (TDUs) were installed instead of the limiter modules of OP 1.1. After OP 1.2b, the whole plasma vessel of W7-X was inspected using a handy digital microscope and a digital camera. The surfaces of interests include first wall panels, in-vessel ports made of SS, and TDUs, plasma facing surfaces of heat shields and baffles made of graphite, and heat sinks of the baffles made of CuCrZr plates and inboard-side vacuum vessel surfaces behind the heat shield and baffles. There were no arc trails observed on the graphite surfaces of TDUs, heat shields and baffles, which is favorable result for a stable operation of the machine. On the other hand, many arc trails were recorded on the other surfaces.

A total of 317 SS panels, several ports and the plasma vessel surfaces were inspected after OP 1.2b. Among them, 55 SS panels were taken out of the vacuum vessel for inspection of their rear side surfaces. W7-X consists of 5 main modules and all the trails observed were classified by their locations and marked onto a 3D CAD model of each module. Figure 5 shows a schematic illustration of the SS panels and TDUs of the module 3. The locations of arc spots detected are marked as red, blue and green circles for front, rear and vessel or port surfaces, respectively. Arcing initiated not only on plasma-facing surfaces, but also rear side of SS panels, CuCrZr cooling structures and deep region of several ports, where the main plasma could

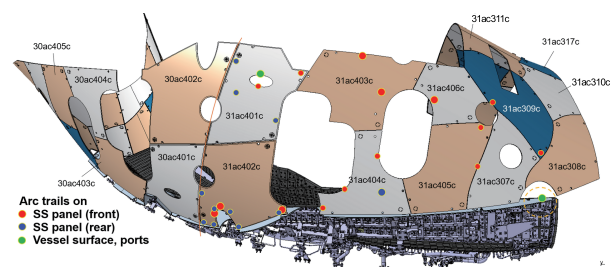


Fig. 5 Mapping of arc trail locations observed on the module 3 of W7-X.

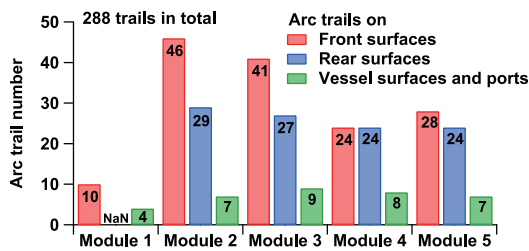


Fig. 6 The number distribution of arc trails on front, rear side SS panels and vessel and port surfaces for each module.

not directly reach. Throughout all the modules, 288 trails were observed. Almost half of the trails (52%) appeared on the front side of SS panels, and 36% and 12% did on the rear side surfaces and the inboard side vessel surfaces including several ports, respectively.

Figure 6 shows the number of arc trails classified by the locations for each module. On the front side surfaces, the number of arc trails varied. The largest amount was 46 trails recorded in the module 2, whereas the smallest number of 10 trails appeared in a neighboring module, the module 1. Rear side arc trails were distributed rather equally, ranging from 24 to 29 trails for each module. Note that rear side surfaces of the module 1 were not investigated. Less than 10 trails were on various ports and inboard side vessel surfaces.

Arcing on rear side surfaces of the SS panels or other shadowed surfaces was unexpected before we inspected. It is unlikely that the main plasma of W7-X impacted those surfaces and initiated arcing. As mentioned above, in general arc spots on a metal surface are affected by an effective external magnetic field existing [17]. During the operation of main plasma discharges, the magnetic field was raised up to 2.5 T, which would make arc trails move toward $-\mathbf{j} \times \mathbf{B}$ direction. Throughout the in-vessel inspection, however, most of arc trails appeared with rather broad, disorganized features.

Figure 7 shows photos of arc trails by a digital camera. Figures 7 (a) and (b) show the arc trails formed on the front side of SS wall panels. Many trails with a length of $\sim 1-10$ cm initiated from edge or the interior of the panels. On the rear side of SS panels, arc trails tended to become broader. Figure 7 (c) shows arc trails recorded on the rear side of a SS panel. The trails were distributed with the length of ~ 30 cm and directed along the curvature of the panel surface while splitting into several branches. Figures 7 (d) and (e) show arc trails formed on a CuCrZr cooling structures and plates of Doppler reflectometry, respectively. For both cases, broad and planar trails were featured. Considering the morphologies of the arc trails, which showed broad, undirected and split motions of arc spots, and the locations of ignition on the rear side surfaces, it is likely that most of arc trails were formed during non-magnetized phases, i.e., glow discharge cleaning phase. On the other hand, some trails had clear orientation.



Fig. 7 Digital camera photos of arc trails on: (a)-(b) SS wall panels (front), (c) SS wall panel (rear), (d) CuCrZr cooling structure, (e) a surface of Doppler reflectometry plates and (f) a surface of infrared/ H_{α} camera insert.

Figure 7 (f) shows arc trails on the surface of infrared/ H_{α} camera port. Several arcs ignited near edges and propagated inside along the cylindrical surface. These trails show clear linearity, thus they could be affected by the external magnetic field. During the OP 1.2b, the general direction of the magnetic field was counter-clockwise looking from the top down to the torus, but operations with clockwise orientation were also performed. Therefore, there is a possibility of the arc ignition during the main plasma discharge.

Arc initiation is usually related to electron emission processes including thermal emission, field emission (cold emission) and/or thermo-field emission taking both into account [20]. Therefore, it is reasonable to think that arcs can more easily ignite at the edges of surfaces, where field emission is enhanced due to locally intensified electric fields. Indeed, a majority of arc trails were detected at the edges of components, typically shown in Fig. 7 (a). Figure 8 shows the number of the arc trails classified by the location and the surface condition. Among 253 arc trails recorded on the SS wall panels, 79% occurred on the edges of the panels and 21% were on the interior of the surfaces. The interior has a planar surface and a flat electric field, thus arcing seems difficult to be initiated. It is noteworthy that almost half (49%) of the arc trails on the interior of the SS panels appeared with a deposition spot (dusty or weld spot, see an example in Fig. 7 (b)). On the other hand, the portion of arc trails with a dusty spot on the edge was only 3.5%. This result indicates that dusty spots acted as a seed

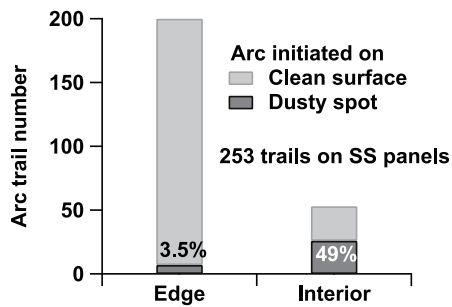


Fig. 8 Arc trail number classified by the location and the surface condition.

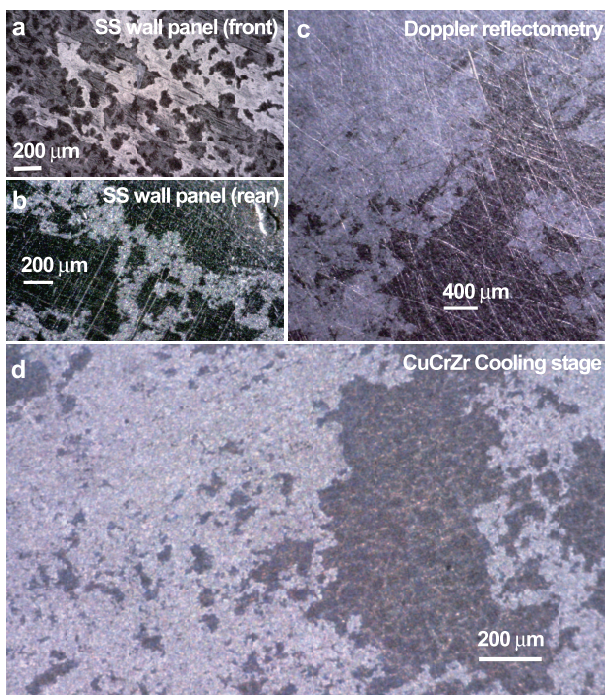


Fig. 9 Digital microscope images of arc trails on: (a) SS wall panel (front), (b) SS wall panel (rear), (c) a surface of Doppler reflectometry plate and (d) CuCrZr cooling structure.

of arc ignition, as explicitly explained in [17, 20].

One of the main effect of arcing on fusion devices is wall erosion. In detailed observation using a handy digital microscope (Dino-lite AM7915MZT), wall erosion by arc trails was detected. Figure 9 shows microscope images of arc trails on various surfaces, such as the front and the rear side of SS panels, surface of the Doppler reflectometry plate (see Fig. 7 (e)) and the CuCrZr cooling structure (see Fig. 7 (d)). It is noticeable that arc trails were sensitive to surface roughness. On rather rough surface as seen in Fig. 9 (a), the arc trails formed on a similar surface, avoiding black-colored dots. When a surface becomes smoother, arc trails also broadened as shown in Figs. 9 (b) and (c), where the plate of Doppler reflectometry was polished.

During the OP 1.2b, arc trails appeared only on SS wall panels and other in-vessel surfaces, not on graphite

PFCs. Therefore, erosion of PFCs and plasma contamination by arcing could be ignored. In turn, arc trails on diagnostics were observed and this can affect the precision and sustainability of diagnostics. Glow discharge cleaning is a necessary process prior to the main plasma operation. Therefore, arc ignition at the glow discharge should be prevented. Finishing the edges with a curved surface, polishing the dusty spots on mirror plates of diagnostics can be one method.

4. Summary

In this research, arc trails on various PFCs in LHD and W7-X were investigated. To clarify the effect of nanostructuring on tungsten, a W-fuzz sample was prepared and exposed to the LHD plasma. After one hydrogen discharge, arc ignited and the arc trails were formed straightforward to the retrograde direction, i.e., $-\mathbf{j} \times \mathbf{B}$ direction. After the annual operation phase of LHD in 2011, several PFCs were taken out of vessel for inspection. Arc trails formed on graphite divertor tiles as well as on the SS first walls, seemingly caused by main discharge operation.

In W7-X, there were severe damages on some of the limiter Langmuir probes after the OP 1.1. Graphite probe tips were evaporated and the SS sleeves were melted, remaining arc trails were seen on their surfaces. The possibility of arcing between the probe tip and grounded surroundings was discussed. After the recent OP 1.2b of W7-X, no arc trails appeared on graphite surfaces in W7-X. In turn, all arcs remained on metallic surfaces. From the first thorough in-vessel inspection for arc trails, ~ 300 trails were observed. A considerable number of the trails appeared on non-plasma exposed regions: the rear side surface of SS panels and CuCrZr cooling structures. Furthermore, a vast majority of the arc trails had no clear linearity of direction, indicating that arcing initiated during glow discharge cleaning phase while a few trails showed linearity. Enhanced electric field and resultant electron emission from the edges of SS panels and deposition/weld spots on the interior of surfaces were pointed out as the main initiator of arcing. For the following work, depth profiling of arc trails is necessary to estimate the erosion amount by arcing and to quantify the degradation of diagnostics by arc trails on the surface.

Acknowledgments

D. Hwangbo would like to thank Dr. G. Motojima and Dr. Y. Hayashi for their cooperation in this investigation. This work was supported in part by a Grant-in-Aid for JSPS Fellows 17J05670, Grant-in-Aid for Scientific Research 15H04229, Grant-in-Aid for Exploratory Research 16K13917, Fund for the Promotion of Joint International Research 17KK0132 and Bilateral Joint Research Project from the Japan Society for the Promotion of Science. This work was also supported in part by NIFS collaborative research program NIFS18KLEF020. This work has been

carried out within the framework of the EUROfusion Consortium and has received funding from the Euratom research and training programme 2014-2018 and 2019-2020 under grant agreement No 633053. The views and opinions expressed herein do not necessarily reflect those of the European Commission.

- [1] G. McCracken and D. Goodall, *Nucl. Fusion* **18**, 537 (1978).
- [2] V. Rohde, M. Balden, N. Endstrasser, U. von Toussaint and ASDEX-U Team, *J. Nucl. Mater.* **438**, S800 (2013).
- [3] V. Rohde, M. Balden and ASDEX-U Team, *Nucl. Mater. Energy* **9**, 36 (2016).
- [4] D.L. Rudakov, C.P. Chrobak, R.P. Doerner, S.I. Krasheninnikov, R.A. Moyer *et al.*, *J. Nucl. Mater.* **438**, S805 (2013).
- [5] T. Akiyama, K. Kawahata, N. Ashikawa, M. Tokitani, S. Okajima *et al.*, *Rev. Sci. Instrum.* **78**, 103501 (2007).
- [6] S. Kajita, T. Hatae, T. Sakuma, S. Takamura, N. Ohno *et al.*, *Plasma Fusion Res.* **7**, 2405121 (2012).
- [7] G. De Temmerman, T. Hirai and R.A. Pitts, *Plasma Phys. Control. Fusion* **60**, 044018 (2018).
- [8] S. Kajita, W. Sakaguchi, N. Ohno, N. Yoshida and T. Saeki, *Nucl. Fusion* **49**, 095005 (2009).
- [9] S. Kajita, T. Yagi, K. Kobayashi, M. Tokitani and N. Ohno, *Res. Phys.* **6**, 877 (2016).
- [10] D. Hwangbo, S. Kajita, N. Ohno and D. Sinelnikov, *IEEE Trans. Plasma Sci.* **45**, 2080 (2017).
- [11] M. Tokitani, S. Kajita, S. Masuzaki, Y. Hirahata, N. Ohno, T. Tanabe and LHD Experiment Group, *Nucl. Fusion* **51**, 102001 (2011).
- [12] D.L. Rudakov, C.P.C. Wong, R.P. Doerner, G.M. Wright, T. Abrams *et al.*, *Phys. Scr.* **T167**, 014055 (2017).
- [13] J. Matějčiček, V. Weinzettl, M. Nilémová, T.W. Morgan, G. De Temmerman *et al.*, *J. Nucl. Mater.* **492**, 204 (2017).
- [14] S. Kajita, M. Fukumoto, M. Tokitani, T. Nakano, Y. Noiri *et al.*, *Nucl. Fusion* **53**, 053013 (2013).
- [15] S. Kajita, S. Takamura and N. Ohno, *Plasma Phys. Control. Fusion* **53**, 074002 (2011).
- [16] R.A. Pitts, S. Bardin, B. Bazylev, M.A. van den Berg, P. Bunting *et al.*, *Nucl. Mater. Energy* **12**, 60 (2017).
- [17] A. Anders, *Cathodic Arcs From Fractal Spots to Energetic Condensation* (Springer, New York, 2008) p. 232.
- [18] T. Sunn Pedersen, T. Andreeva, H.S. Bosch, S. Bozhnikov, F. Effenberg *et al.*, *Nucl. Fusion* **55**, 126001 (2015).
- [19] R. König, J. Baldzuhn, W. Biel, C. Biedermann, H.S. Bosch *et al.*, *J. Instrumentation* **10**, P10002 (2015).
- [20] G.A. Mesyats, *Cathode Phenomena in a Vacuum Discharge* (Nauka Publishers, Moscow, 2000) p. 60.
- [21] H. Craig Miller, *IEEE Trans. Electrical Insulation* **24**, 765 (1989).
- [22] T. Sunn Pedersen, R. König, M. Jakubowski, M. Krychowiak, D. Gradic *et al.*, *Nucl. Fusion* **59**, 096014 (2019).
- [23] A.S. Pillai and R. Hackam, *J. Appl. Phys.* **58**, 146 (1985).